© 2017. Published by The Company of Biologists Ltd | Development (2017) 144, 2021-2031 doi:10.1242/dev.145144

RESEARCH ARTICLE

Negative regulation of endothelin signaling by SIX1 is required for proper maxillary development

Andre L. P. Tavares[1], Timothy C. Cox[2], Robert M. Maxson[3], Heide L. Ford[4] and David E. Clouthier[1,*]

ABSTRACT

Jaw morphogenesis is a complex event mediated by inductive signals that establish and maintain the distinct developmental domains required for formation of hinged jaws, the defining feature of gnathostomes. The mandibular portion of pharyngeal arch 1 is patterned dorsally by Jagged-Notch signaling and ventrally by endothelin receptor A (EDNRA) signaling. Loss of EDNRA signaling disrupts normal ventral gene expression, the result of which is homeotic transformation of the mandible into a maxilla-like structure. However, loss of Jagged-Notch signaling does not result in significant changes in maxillary development. Here we show in mouse that the transcription factor SIX1 regulates dorsal arch development not only by inducing dorsal *Jag1* expression but also by inhibiting endothelin 1 (*Edn1*) expression in the pharyngeal endoderm of the dorsal arch, thus preventing dorsal EDNRA signaling. In the absence of SIX1, but not JAG1, aberrant EDNRA signaling in the dorsal domain results in partial duplication of the mandible. Together, our results illustrate that SIX1 is the central mediator of dorsal mandibular arch identity, thus ensuring separation of bone development between the upper and lower jaws.

KEY WORDS: Endothelin, Craniofacial, Neural crest cell, Hinge and caps, Knockout mouse

INTRODUCTION

Development of the vertebrate face requires the coordinated regulation of patterning cues throughout the pharyngeal arches of the developing embryo. Populated by cranial neural crest cells (NCCs) originating in the dorsal neural tube (Le Douarin, 1982; Noden, 1983), NCCs receive patterning signals from the surrounding arch ectoderm and endoderm that establish their positional identity (Clouthier et al., 2010, 2013; Medeiros and Crump, 2012), dividing the arches into dorsal (proximal), intermediate and ventral (distal) domains (Clouthier et al., 2010; Clouthier and Schilling, 2004; Medeiros and Crump, 2012).

Patterning in the intermediate and ventral domains of the mandibular portion of arch 1 is established in large part by endothelin receptor A (EDNRA) signaling within NCCs, arising when arch ectoderm-derived endothelin 1 (EDN1) binds to the EDNRAs on NCCs (Clouthier et al., 1998; Nair et al., 2007; Tavares et al., 2012). This signaling initiates a gene expression cascade that establishes the identity of NCCs in the intermediate/ventral mandibular arch and results in the formation of lower jaw and middle ear structures. Loss of EDNRA signaling leads to homeotic transformation of the mandibular bone into a maxilla-like structure along with other dorsal-ventral duplications (Kimmel et al., 2003; Ozeki et al., 2004; Ruest et al., 2004), events that are preceded by disrupted expression of EDNRA signaling network genes and a ventral expansion of a dorsal domain gene expression profile (Alexander et al., 2011; Clouthier et al., 1998, 2000; Miller et al., 2003; Nair et al., 2007; Ozeki et al., 2004; Ruest et al., 2004; Sato et al., 2008b). This expansion is achieved in part through upregulated Jagged-Notch signaling, the mechanism reported to be responsible for establishing dorsal NCC identity in zebrafish (Zuniga et al., 2010). In this model, Ednra signaling normally represses *jag1b* expression (Zuniga et al., 2011, 2010), while Jagged-Notch signaling prevents expansion of Ednra-dependent gene expression into the dorsal arch (Barske et al., 2016; Zuniga et al., 2010).

Although *Edn1* expression is not observed rostral to the mandibular arch (Clouthier et al., 1998), aberrant EDNRA signaling in maxillary NCCs leads to homeotic transformation of the maxilla into a mandible-like structure (Sato et al., 2008b; Tavares and Clouthier, 2015). These changes are accompanied by an upregulation of a ventral/intermediate gene expression profile in the dorsal mandibular arch domain and maxillary prominence (Sato et al., 2008b; Tavares and Clouthier, 2015; Zuniga et al., 2011). By contrast, overexpression of *jag1b* in zebrafish embryos results in downregulation of ventral arch gene expression (Zuniga et al., 2010). However, unlike changes observed in more caudal arches, loss of *jag1b* expression in zebrafish does not lead to homeotic transformation of dorsal structures in arch 1 (Barske et al., 2016; Zuniga et al., 2010). Similarly, conditional inactivation of *Jag1* in mouse NCCs leads to the development of a shortened maxilla but not to homeotic changes (Humphreys et al., 2012).

The transcription factor SIX1, a member of the SIX family of transcription factors (Kawakami et al., 2000; Kumar, 2009), is involved in numerous developmental and disease-related events, with loss of SIX1 leading to defects in eye, ear, heart, rib, kidney and lower jaw development (Laclef et al., 2003; Ozaki et al., 2004; Xu et al., 2003; Zou et al., 2006, 2004; Guo et al., 2011). In humans, both SIX1 and its co-factor EYA1 have been implicated in branchiootic syndrome [BOS1, Online Mendelian Inheritance in Man (OMIM) 602588; and BOS3, OMIM 608389] and branchiootorenal syndrome (BOR1, OMIM 113650) (Lee et al., 2007; Orten et al., 2008; Ruf et al., 2003, 2004). These syndromes are characterized by hearing loss, defects in pharyngeal arch derivatives and renal anomalies. SIX1 is also involved in the metastatic progression of breast cancer cells and does so through the activation of several signaling networks, including Jagged-Notch signaling (Smith et al., 2012). SIX1 regulates otic vesicle and olfactory epithelium development in a

[1]Department of Craniofacial Biology, University of Colorado Anschutz Medical Campus, Aurora, CO 80045, USA. [2]Department of Pediatrics (Craniofacial Medicine), University of Washington, and Center for Developmental Biology & Regenerative Medicine, Seattle Children's Research Institute, Seattle, WA 98101, USA. [3]Department of Biochemistry and Molecular Biology and Norris Cancer Center, University of Southern California, Los Angeles, CA 87654, USA. [4]Department of Pharmacology, University of Colorado Anschutz Medical Campus, Aurora, CO 80045, USA.

*Author for correspondence (david.clouthier@ucdenver.edu)

D.E.C., 0000-0002-2008-477X

Received 27 September 2016; Accepted 18 April 2017

Development (2017) 144, 2021-2031 doi:10.1242/dev.145144

similar manner (Bosman et al., 2009; Ikeda et al., 2010). This raises the intriguing possibility that SIX1 establishes or maintains Jagged-Notch signaling during pharyngeal arch development.

To investigate this hypothesis, we have examined the function of SIX1 and its relationship to both EDNRA and Jagged-Notch signaling during jaw morphogenesis in mouse. We find that the loss of *Six1* leads to expansion of the maxilla into a rod-shaped bone, with the posterior end of the bone resembling a mandibular process. The formation of this bone occurs in part due to EDNRA signaling in the dorsal mandibular arch that arises from aberrant expression of endodermal pouch-expressed *Edn1*. Therefore, a primary function of SIX1 appears to be maintaining a dorsal mandibular arch domain that is free of EDNRA signaling to ensure that the region between the maxillary prominence and mandibular arch develops without intrusion of bone structures from the maxillary prominence.

RESULTS

Loss of *Six1* leads to the formation of a novel bone in the zygomatic arch

To analyze SIX1 function in facial morphogenesis, we first examined embryos from one of two *Six1* mutant strains that have been created, in which both exons of *Six1* were targeted (Ozaki et al., 2004). Control and $Six1^{-/-}$ embryos were first collected at embryonic day (E) 18.5 and skull structures analyzed by both Alizarin Red/Alcian Blue staining (Fig. 1A-D′) and micro-computed tomography (micro-CT) (Fig. 1E,F). $Six1^{-/-}$ embryos presented with retrognathia (Fig. 1B,D) and previously described defects in the nasal bones, otic capsule, tympanic ring bone and middle ear ossicles (Fig. 1B) (Guo et al., 2011; Ozaki et al., 2004). However, the most striking change in $Six1^{-/-}$ embryos was the formation of a novel bone extending posteriorly from the maxilla. In mice, the zygomatic arch is normally composed of the zygomatic process of the maxilla, the jugal bone and the zygomatic process of the squamosal bone (Fig. 1A,C,C′ and pseudo-colored red, blue and green, respectively, in 1E). In $Six1^{-/-}$ embryos, the anterior portion of the maxilla appeared similar to that of control embryos (Fig. 1B,D,D′,F). However, the zygomatic process of the maxilla became a thicker and longer rod-shaped bone (arrowhead in Fig. 1D,D′ and pseudo-colored red in 1F; arrowheads in 1F) and was capped in cartilage (arrows in Fig. 1B,D,D′), similar to mandibular processes (Fig. 1B,D). The jugal bone was present as a separate element or fused to the new maxillary bone (pseudo-colored blue in Fig. 1F).

The condylar process of the mandible rests in the mandibular fossa of the squamosal bone, with these two structures comprising the temporomandibular joint (TMJ). The articular disk rests between these two bones (Hanken and Hall, 1993). In $Six1^{-/-}$ embryos, the anterior end of the elongated bone ended at the mandibular fossa. In addition, whereas the articular disk overlaid the condylar process of the mandible in both control (Fig. 1G) and $Six1^{-/-}$ (Fig. 1H) embryos, the disk in mutant embryos bifurcated to also extend over the posterior end of the elongated bone (Fig. 1H, arrow). These findings suggest that loss of SIX1 leads to a partial transformation of the proximal maxilla into a structure, the posterior end of which resembles the posterior mandible. Although defects in the maxilla were not reported in the other *Six1* mutant strain (Laclef et al., 2003), different targeting strategies and mouse genetic background could influence phenotypic penetrance.

Loss of *Six1* disrupts expression of maxillary patterning genes

Misexpression of *Edn1* in NCCs within the maxillary prominence results in complete homeotic transformation of the maxilla into a mandible (Sato et al., 2008a; Tavares and Clouthier, 2015). One method we have previously used to achieve this misexpression was through conditional activation of *Edn1* expression in NCCs (Tavares and Clouthier, 2015) (Fig. 2C,C′) (see Materials and Methods). Interestingly, the bifurcation of the posterior end of the novel maxillary bone in $Six1^{-/-}$ embryos (Fig. 2B-B″) resembled the posterior end of the duplicated mandible in *CBA-Edn1;Wnt1-Cre* embryos (Fig. 2C-C″). For reference, the jugal bone was not bifurcated in control embryos (Fig. 2A-A″). To determine whether the maxillary changes reflected earlier changes in NCC patterning (Clouthier et al., 2010, 2013; Medeiros and Crump, 2012), we examined gene expression in E10.5 control and $Six1^{-/-}$ embryos. As a positive control for expanded EDNRA signaling, we also examined gene expression in *CBA-Edn1;Wnt1-Cre* embryos.

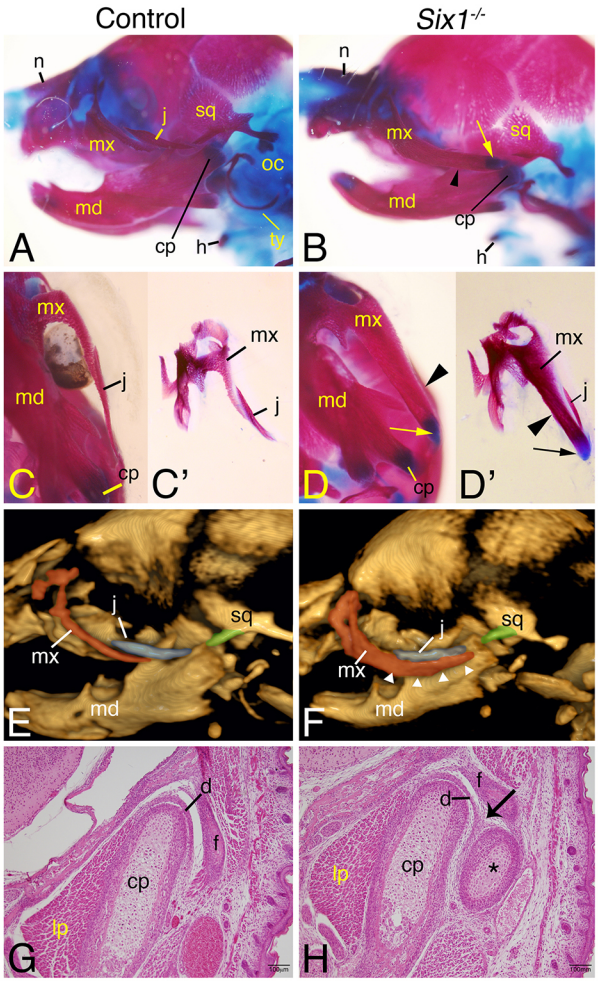

Fig. 1. Analysis of craniofacial defects in E18.5 $Six1^{-/-}$ mouse embryos. (A-D′) Alizarin Red (bone) and Alcian Blue (cartilage) staining of control (left column) and $Six1^{-/-}$ (right column) embryos. Representative embryos are shown in lateral (A,B) and ventral (C,C′,D,D′) views. In $Six1^{-/-}$ embryos, the maxilla (mx) extends posteriorly as a rod-shaped bone (arrowhead) that is capped in cartilage (arrow) (B,D,D′). Control, *n*=10; $Six1^{-/-}$, *n*=8. (E,F) Micro-CT scans of control (E) and $Six1^{-/-}$ (F) embryos. The maxilla (red), jugal (blue) and zygomatic process of the squamosal (green) bones are pseudo-colored. Arrowheads denote elongated bone. (G,H) Hematoxylin and Eosin-stained frontal sections through the TMJ. In $Six1^{-/-}$ embryos, the end of the elongated maxillary bone (asterisk) resides within the mandibular fossa (f) and is covered in cartilage. In addition, the articular disk (d) bifurcates to also contact the elongate bone (arrow in H). Control, *n*=4; $Six1^{-/-}$, *n*=4. Scale bars: 100 µm. cp, condylar process; h, hyoid; j, jugal bone; lp, lateral pterygoid muscle; md, mandible; n, nasal bone; oc, otic capsule; sq, squamosal bone; ty, tympanic ring.

Development (2017) 144, 2021-2031 doi:10.1242/dev.145144

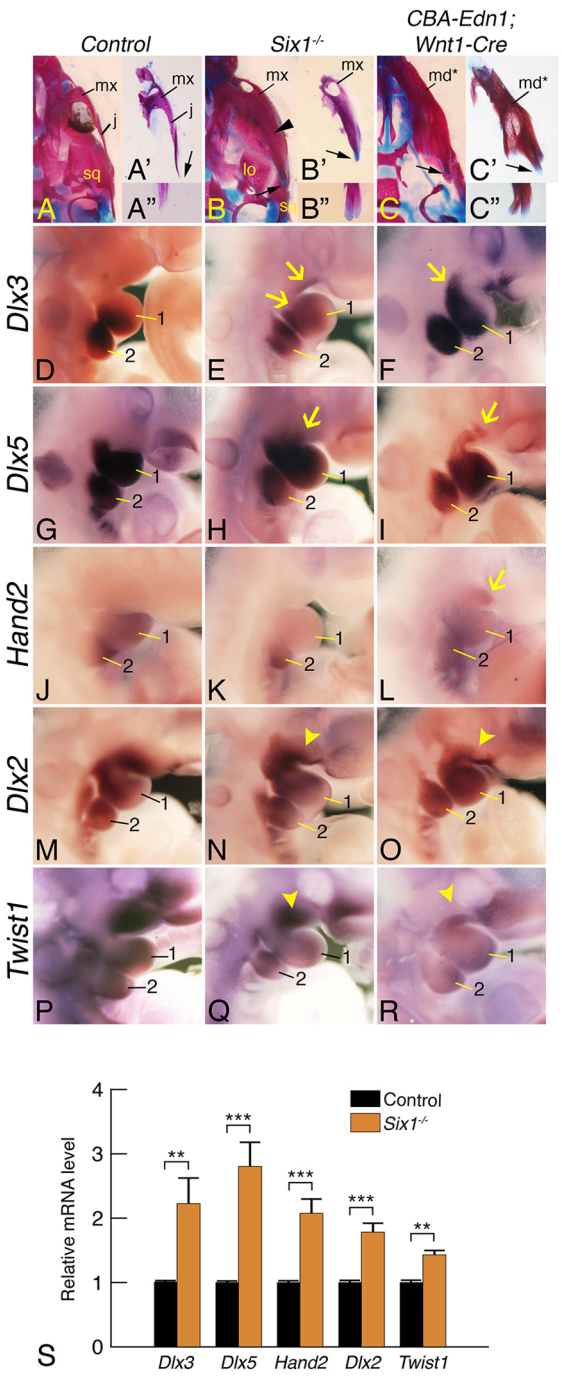

Fig. 2. Similarities in facial structures and earlier gene expression patterns between *Six1*$^{-/-}$ and *CBA-Edn1;Wnt1-Cre* embryos. (A-C′′) Ventral view of representative E18.5 embryo skulls (A-C) and dissected views of the control maxilla (A′,A″), elongated bone in *Six1*$^{-/-}$ embryos (arrowhead in B′;B″) and duplicated mandible in *CBA-Edn1;Wnt1-Cre* embryos (C′,C″). Rotation of the dissected bones reveals two processes capped in cartilage (arrows) on the proximal end of the elongated bone (B″) and duplicated mandible (C″). Control, *n*=10; *Six1*$^{-/-}$, *n*=8; *CBA-Edn1;Wnt1-Cre*, *n*=7. (D-R) Whole-mount ISH analysis of gene expression in E10.5 control (D,G,J,M,P), *Six1*$^{-/-}$ (E,H,K,N,Q) and *CBA-Edn1;Wnt1-Cre* (F,I,L,O,R) embryos. Arrows indicate regions of expanded gene expression; arrowheads indicate regions of reduced gene expression. (S) Quantification of gene expression in the proximal mandibular arch of control and *Six1*$^{-/-}$ embryos. *n*=3; error bars represent s.e.m.; two-tailed *t*-test, ***P*<0.01, ****P*<0.001. 1, first pharyngeal arch; 2, second pharyngeal arch; j, jugal; lo, lamina obturans; md*, duplicated mandible; mx, maxilla; sq, squamosal bone. The images shown are representative of three embryos of each genotype.

Expression of *Dlx3* (Fig. 2D-F), an intermediate domain marker (Tavares et al., 2012; Walker et al., 2006), and *Dlx5* (Fig. 2G-I), a dorsal/intermediate marker (Talbot et al., 2010; Tavares et al., 2012), expanded into both the rostral mandibular arch and maxillary prominence in both *Six1*$^{-/-}$ (Fig. 2E,H) and *CBA-Edn1;Wnt1-Cre* (Fig. 2F,I) (Tavares and Clouthier, 2015) embryos. By contrast, aberrant *Hand2* expression was not observed in the dorsal mandibular arch or maxillary prominence (Fig. 2K), although expression was decreased in the ventral mandibular arch (Fig. 2K and data not shown). In *CBA-Edn1;Wnt1-Cre* embryos, expanded *Hand2* expression was observed in the maxillary prominence (Fig. 2L).

Loss of EDNRA signaling also results in ventral expansion of *Dlx2* and *Twist1* (Ruest et al., 2004). In both *Six1*$^{-/-}$ and *CBA-Edn1;Wnt1-Cre* embryos, the expression of *Dlx2* (Fig. 2M-O) and *Twist1* (Fig. 2P-R) was reduced in the maxillary prominence of *Six1*$^{-/-}$ embryos (Fig. 2N,Q), although the reduction was less severe than that observed in *CBA-Edn1;Wnt1-Cre* embryos (Fig. 2O,R). To quantify these changes, we used quantitative real-time PCR (qRT-PCR) analysis to assay the levels of gene expression in the dorsal mandibular arch of E10.5 embryos. Compared with control embryos, the expression of all five genes was significantly upregulated in *Six1*$^{-/-}$ embryos (Fig. 2S), indicating an upregulation of ventral gene expression in this region. It is important to note that the graph only depicts the relative expression of each gene between genotypes and does not reflect the level of expression between genes. Although *Hand2* expression was elevated, as indicated by qRT-PCR, the relative expression was 50% lower than that of the other genes (data not shown). Together, these results illustrate that the *Six1*$^{-/-}$ phenotype is likely to result from similar changes in early NCC patterning as observed after *Edn1* overexpression.

EDNRA and SIX1 genetically interact during NCC patterning

Owing to similarities in both phenotypic and gene expression changes in *Six1*$^{-/-}$ and *CBA-Edn1;Wnt1-Cre* embryos, we analyzed the expression of *Six1* and its co-factor *Eya1* in E10.5 *CBA-Edn1;Wnt1-Cre* and *Ednra*$^{-/-}$ embryos. In control embryos, *Six1* (Fig. 3A) and *Eya1* (Fig. 3E) were both expressed in the maxillary prominence, with *Six1* expression also prominent in the dorsal mandibular arch adjacent to the first pharyngeal pouch (arrowhead in Fig. 3A). Expanded EDNRA signaling in *CBA-Edn1;Wnt1-Cre* embryos disrupted the expression of both *Six1* and *Eya1* in the maxillary prominence (Fig. 3B,F), with expression in the dorsal mandibular arch also decreased (arrowhead in Fig. 3B). By contrast, expression of both *Six1* and *Eya1* appeared to be expanded in the ventral mandibular arch in *Ednra*$^{-/-}$ embryos (Fig. 3C,G), with dorsal arch expression of *Six1* appearing similar to that in controls (arrowhead in Fig. 1C). We also examined *Six1/Eya1* expression in E10.5 *Jag1*$^{fl/fl}$*;Wnt1-Cre* embryos, in which *Jag1* expression was conditionally deleted in NCCs. For both genes, expression did not appear dramatically changed (Fig. 3D,H); this included the *Six1* expression domain in the dorsal mandibular arch (arrowhead in Fig. 3D). These results suggest that *Six1/Eya1* expression in the dorsal mandibular arch is not repressed by Jagged-Notch signaling during early arch patterning. We therefore examined *Edn1* expression in E9.5 control and *Six1*$^{-/-}$ embryos, comparing it with *Six1* expression. At this age, *Six1* expression in control embryos was observed in the pharyngeal pouch endoderm and in the arch mesenchyme (Fig. 3I,I′). This inversely corresponded to areas of highest *Edn1* expression in control embryos, observed in the arch endoderm (Fig. 3J,J′); expression in pouch endoderm and arch

Development (2017) 144, 2021-2031 doi:10.1242/dev.145144

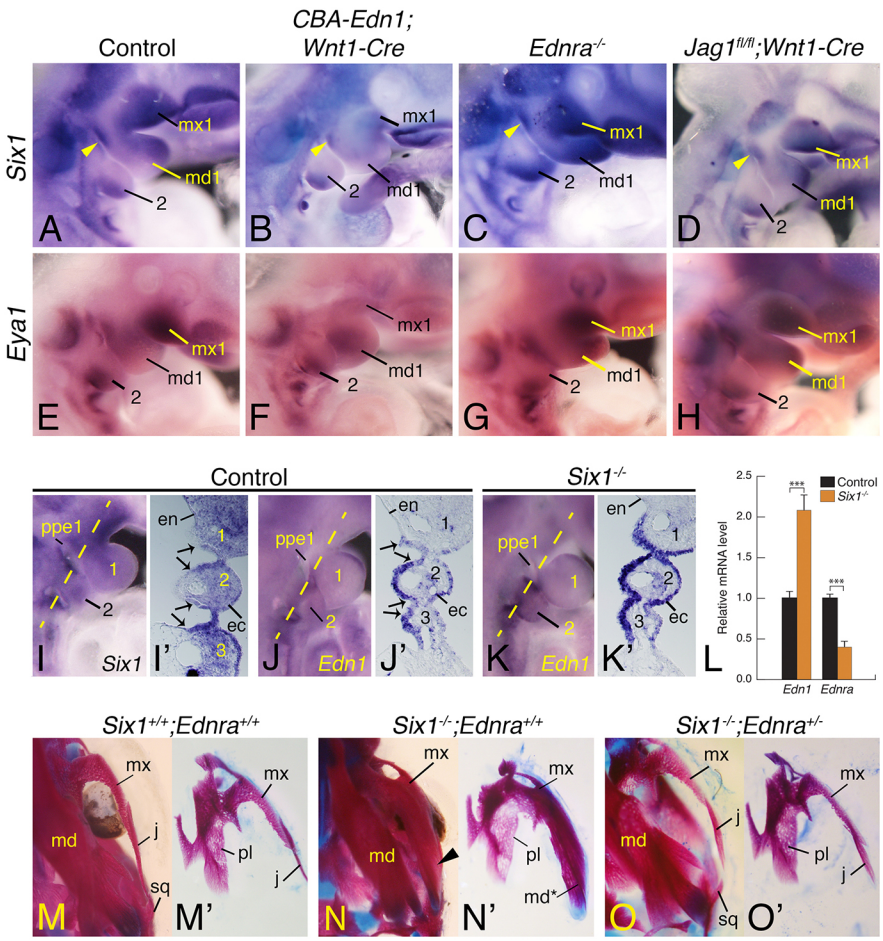

Fig. 3. Genetic interaction between *Six1* and *Ednra*. (A-H) Whole-mount ISH analysis of *Six1* and *Eya1* expression in E10.5 control (A,E), *CBA-Edn1;Wnt1-Cre* (B,F), *Ednra*$^{-/-}$ (C,G) and *Jag1*$^{fl/fl}$*;Wnt1-Cre* (D,H) embryos. The *Six1* expression domain in the dorsal mandibular arch is marked by yellow arrowheads. (I-K′) Analysis of E9.5 embryos following whole-mount (I,J,K) or sectional (I′,J′,K′) ISH. The plane of section for I′,J′,K′ is depicted by the dashed yellow lines on I,J,K, respectively. *Six1* expression in control embryos is strongest in the pharyngeal pouch endoderm (en) of arches 1 and 2 (demarcated by arrows) (I,I′). *Edn1* is expressed along the pharyngeal endoderm of control embryos, but is weaker in pharyngeal pouch endoderm (demarcated by arrows) (J,J′). *Edn1* expression is enhanced in the endoderm and ectoderm (ec) of *Six1*$^{-/-}$embryos (K,K′). The images shown are representative of three embryos of each genotype. (L) Quantification of *Edn1* and *Ednra* expression in the proximal mandibular arch of E10.5 control and *Six1*$^{-/-}$ embryos. *n*=3; error bars represent s.e.m.; two-tailed *t*-test, ***P<0.001. (M-O′) Ventral view of E18.5 skulls from a *Six1;Ednra* allelic series shown in ventral (M,N,O) and dissected ventral (M′,N′,O′) views. The elongated bone observed in *Six1*$^{-/-}$*;Ednra*$^{+/+}$ embryos is denoted by an arrowhead. *Six1*$^{+/+}$*;Ednra*$^{+/+}$, *n*=10; *Six1*$^{-/-}$*;Ednra*$^{+/+}$, *n*=8; *Six1*$^{-/-}$*;Ednra*$^{+/-}$, *n*=7. md1, mandibular arch 1; mx1, maxillary prominence of arch 1; 1, arch 1; 2, arch 2; 3, arch 3; j, jugal; md, mandible; mx, maxilla; pl, palatine bone; ppe1, pharyngeal pouch endoderm; sq, squamosal bone.

ectoderm was weaker (Fig. 3J′). In E9.5 *Six1*$^{-/-}$ embryos, ectodermal and endodermal *Edn1* expression was increased in arches 1 and 2 (Fig. 3K,K′). To better quantify this change, qRT-PCR was used to assay the level of *Edn1* expression in the dorsal mandibular arch of E10.5 embryos. Compared with control embryos, *Edn1* expression was elevated ∼2-fold in *Six1*$^{-/-}$ embryos (Fig. 3L). Interestingly, the expression of *Ednra* was ∼50% lower, indicating that receptor levels might compensate for changes in ligand levels.

These reciprocal changes in gene expression suggest a genetic interaction between SIX1 and EDNRA. To test whether such an interaction exists, we examined whether reducing *Ednra* gene dosage would rescue the *Six1*$^{-/-}$ maxillary phenotype (Fig. 3N,N′). Removing one *Ednra* allele on the *Six1*$^{-/-}$ background completely rescued maxillary development in 42% (3/7) of *Six1*$^{-/-}$*;Ednra*$^{+/-}$ embryos (Fig. 3O,O′), with the maxilla resembling the maxilla of control embryos (Fig. 3M,M′). In the remaining *Six1*$^{-/-}$*;Ednra*$^{+/-}$ embryos, no change in the *Six1*$^{-/-}$ phenotype was observed, arguing the existence of modifier or background effects (data not shown). The maxillary defect was observed in 11/12 *Six1*$^{-/-}$ embryos examined (1/12 embryos had the defect on only one side), arguing that variable penetrance was not a major factor in the degree of phenotypic rescue. Removing an additional *Ednra* allele resulted in a rescue percentage of 100% (2/2) in *Six1*$^{-/-}$*;Ednra*$^{-/-}$ embryos, although the significant defects in lower jaw development complicated analyses of these embryos (data not shown).

SIX1 is required for proper Jagged-Notch signaling

Jagged-Notch signaling patterns dorsal NCCs in the zebrafish arches, in part by repressing Ednra signaling (Zuniga et al., 2010). Because *Six1* expression appeared normal in *Jag1*$^{fl/fl}$*;Wnt1-Cre* mouse embryos, we examined whether a relationship exists between SIX1 and Jagged-Notch signaling that influences EDNRA signaling by analyzing the expression patterns of *Jag1*, *Notch1*, *Notch2* and *Hey1* in E9.5 and E10.5 control and *Six1*$^{-/-}$ embryos. *Jag1* expression in control embryos was first detected at E9.5 in the endoderm of pharyngeal pouches 1 and 2 (Fig. 4A,A′); expression was similar in E10.5 control embryos (Fig. 4C), although expression extended into the arch mesenchyme adjacent to the pharyngeal endoderm of arch 1 (Fig. 4C′). In *Six1*$^{-/-}$ embryos, expression of *Jag1* was decreased in pouch endoderm at E9.5 (Fig. 4B,B′) and in arch 1 mesenchyme at E10.5 (Fig. 4D,D′). *Notch1* was weakly expressed in the first arch at both time points in control (Fig. 4E,G) and *Six1*$^{-/-}$ (Fig. 4F,H) embryos. By contrast, *Notch2* expression in E9.5 control (Fig. 4I) and *Six1*$^{-/-}$ (Fig. 4J) embryos was detected in the first arch, with expression increased by E10.5 in the mesenchyme of the mandibular and maxillary regions of the first arch in both genotypes (Fig. 4K,L). Finally, expression of the Jagged-Notch mediator *Hey1* was observed in a small area of the dorsal (hinge) mandibular arch mesenchyme that partially overlapped with the *Jag1* expression domain at E9.5 (Fig. 4M,M′), and this *Hey1* expression domain expanded at E10.5 (Fig. 4O,O′). Expression was decreased in *Six1*$^{-/-}$ embryos at E9.5 (Fig. 4N,N′) and E10.5 (Fig. 4P,P′). Quantitation of the *Hey1* expression area in E10.5 *Six1*$^{-/-}$ embryos revealed a ∼70% decrease compared with the expression area in control embryos (Fig. 4Q).

We also examined gene expression using qRT-PCR with RNA isolated from the dorsal half of the mandibular arch of E9.5 (Fig. 4R) and E10.5 (Fig. 4S) control and *Six1*$^{-/-}$ embryos. At E9.5,

Development (2017) 144, 2021-2031 doi:10.1242/dev.145144

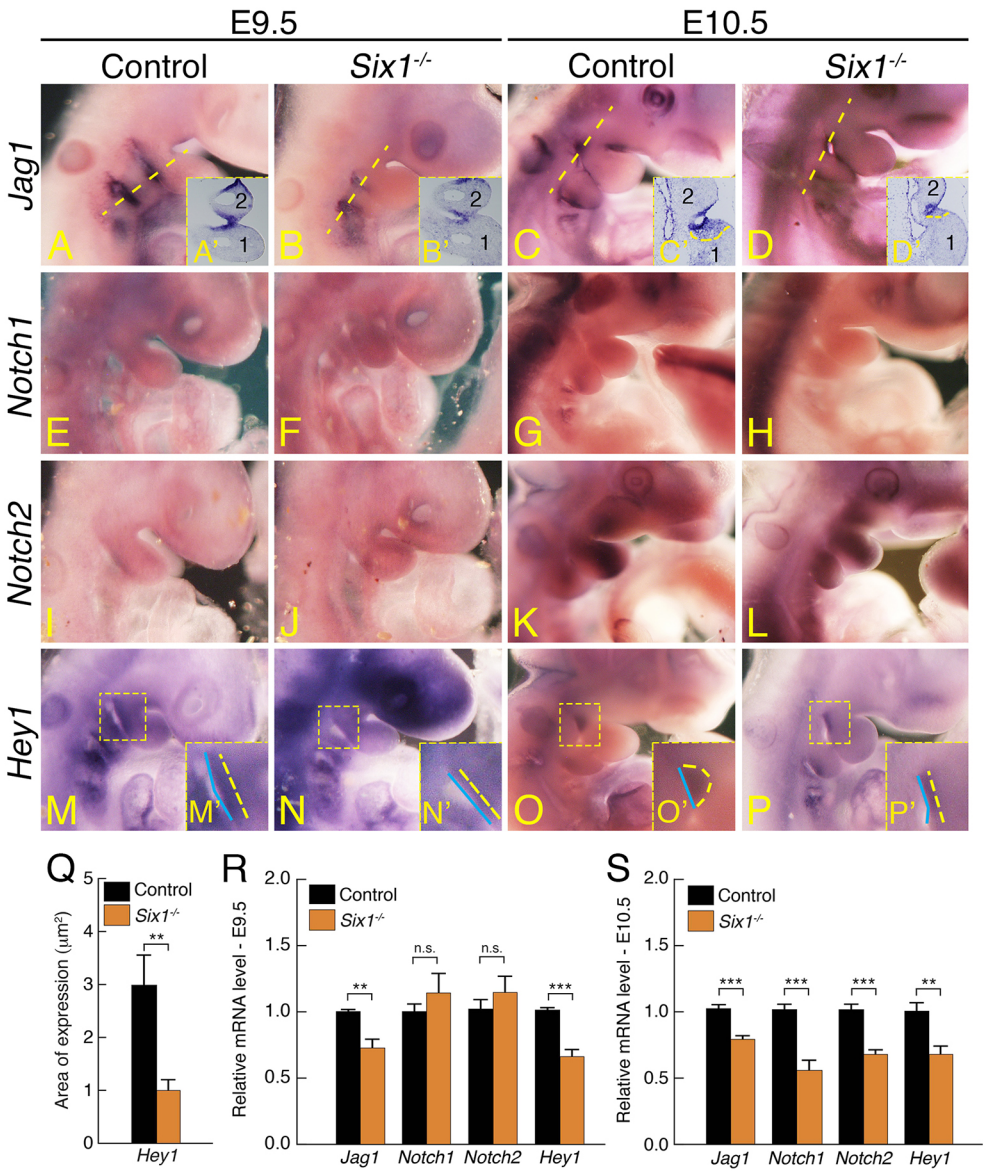

Fig. 4. SIX1 is required for proper *Jag1* expression in the hinge region. (A-P′) Whole-mount ISH analysis of *Jag1* (A-D), *Notch1* (E-H), *Notch2* (I-L) and *Hey1* (M-P) in E9.5 (A,B,E,F,I,J,M,N) and E10.5 (C,D,G,H,K,L,O,P) embryos. (A′-D′) Section ISH of *Jag1* expression; the plane of section is depicted by the dashed yellow lines in A-D. 1, arch 1; 2, arch 2. (M′-P′) Magnification of the boxed area shown in M-P. Blue lines demarcate the pharyngeal endoderm; dashed yellow lines demarcate the extent of *Hey1* expression in the arch mesenchyme. The images shown are representative of four embryos of each genotype subjected to ISH. (Q) Quantification of the *Hey1* expression domain in control and *Six1*$^{-/-}$ embryos shown in O-P′. *n*=4. (R,S) Quantification of mRNA levels in the dorsal mandibular arch of E9.5 (R) and E10.5 (S) control and *Six1*$^{-/-}$ embryos. *n*=3. Error bars represent s.e.m.; two-tailed *t*-test, ***P*<0.01, ****P*<0.001, n.s., not significant.

expression of both *Jag1* and *Hey1* had decreased 30-40%, whereas expression of *Notch1* and *Notch2* did not significantly differ between genotypes. These findings mirrored those observed in *in situ* hybridization (ISH) analysis. At E10.5, *Jag1* expression had decreased by ∼25%, whereas expression of *Notch1*, *Notch2* and *Hey1* had decreased 40-50% (Fig. 4S). Although the *Jag1* and *Hey1* results match those observed in ISH, the decrease in *Notch1* and *Notch2* suggests that expression changes are present in the dorsal mandibular arch but are below the sensitivity of ISH. Overall, these findings indicate that loss of SIX1 adversely affects Jagged-Notch signaling in the dorsal mandibular arch.

To further investigate the relationship between SIX1 and Jagged-Notch signaling, a *Six1* expression construct was transfected into the mouse NCC line O9-1, with expression levels of Jagged-Notch and EDNRA signaling components subsequently assessed by qRT-PCR (Fig. 5A). Overexpression of *Six1* resulted in a significant increase in *Jag1* and *Notch2* mRNA levels, whereas changes in *Notch1* expression were not statistically significant. These findings support the idea that SIX1 regulates Jagged-Notch signaling. Similarly, expression of *Six1* led to significant downregulation of *Dlx3* and *Dlx5* expression. In addition, *Edn1* expression was also downregulated whereas expression of *Ednra* was upregulated (Fig. 5A). This pattern is opposite to that observed in *Six1*$^{-/-}$ embryos (Fig. 2E,H and Fig. 3K,L) and again indicates that SIX1 functions in part through regulating EDNRA signaling, most likely by regulating *Edn1* expression.

While loss of SIX1 resulted in downregulation of *Jag1* expression and upregulation of *Edn1* expression, it is possible that decreased *Jag1* expression was primarily caused by elevated EDNRA signaling as observed during normal intermediate/ventral mandibular arch patterning (Zuniga et al., 2010). To test this possibility, we examined whether SIX1 could induce *Jag1* expression in the presence of EDN1 (Fig. 5B). We found that the addition of EDN1 to *Six1*-transfected cells prevented upregulation of *Jag1* expression (Fig. 5B), suggesting that a key component of SIX1 induction of *Jag1* expression is the repression of *Edn1* expression.

Loss of SIX1 affects gene expression in the hinge region

Because loss of *Six1* disrupts normal development of the posterior maxilla, we examined the expression of genes previously identified as playing a role in the development of this region. Zygomatic arch

Development (2017) 144, 2021-2031 doi:10.1242/dev.145144

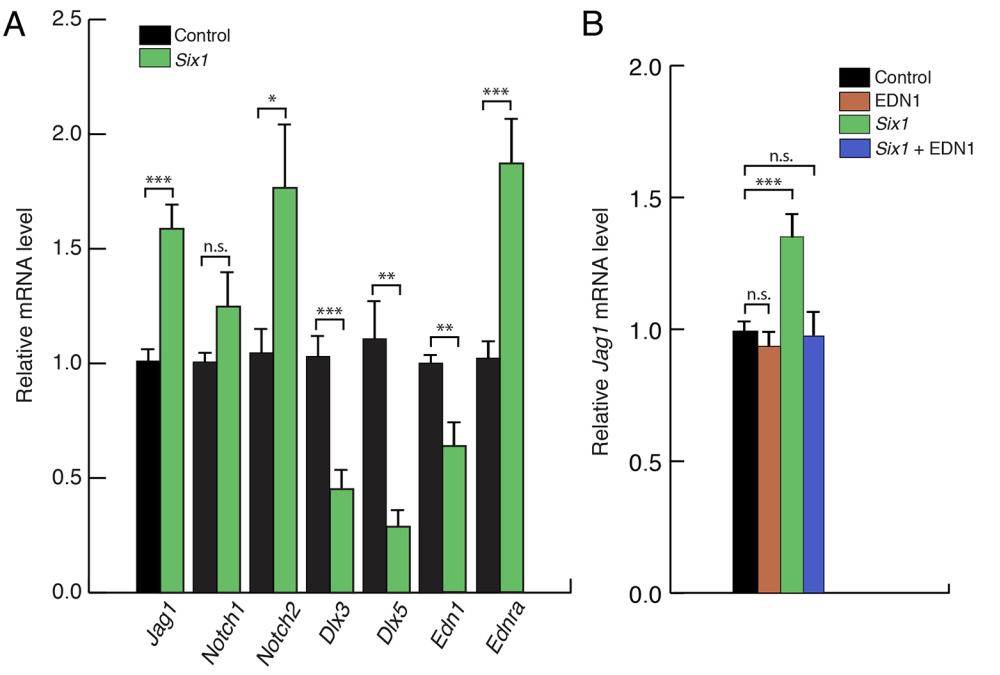

Fig. 5. SIX1 regulates *Edn1* and *Jag1* expression independently. (A) qRT-PCR analysis of gene expression in O9-1 cells following transfection of either a control vector or a *Six1* expression vector. (B) qRT-PCR analysis of gene expression changes in O9-1 cells following transfection with a *Six1* expression vector, treatment with EDN1, or both transfection with a *Six1* expression vector and treatment with EDN1. n=3; error bars represent s.e.m.; two-tailed t-test *P<0.05, **P<0.01, ***P<0.001.

development requires PRRX1 and PRRX2 (Lu et al., 1999; ten Berge et al., 1998). Similarly, Prrx1a/b has recently been shown to work in parallel with Jagged-Notch signaling to pattern the dorsal region of zebrafish pharyngeal arches (Barske et al., 2016). This function involves Barx1, a protein that is required for zebrafish jaw joint formation (Nichols et al., 2013). In E10.5 control mouse embryos, *Prrx1*, *Prrx2* and *Barx1* were expressed in a similar fashion in the maxillary prominence and in the ventral and intermediate domains of the mandibular arch (Fig. 6A,D,G). Expression of each was excluded from the dorsal mandibular arch domain. In *Six1*$^{-/-}$ embryos, the expression of all three genes expanded into the dorsal region (Fig. 6B,E,H). In *CBA-Edn1;Wnt1-Cre* embryos, expression of *Prrx1* (Fig. 6C) and *Barx1* (Fig. 6I) had also expanded into the dorsal domain, even though there was a partial downregulation in the maxillary prominence. By contrast, *Prrx2* (Fig. 6F) was downregulated in the maxillary prominence, suggesting that its upregulation in *Six1*$^{-/-}$ embryos is likely to be EDNRA independent. We also analyzed *Pou3f3*, the expression of which normally spans the maxillary prominence and dorsal mandibular arch (Fig. 6J). Expression of this gene was completely downregulated in *CBA-Edn1;Wnt1-Cre* embryos (Fig. 6L) and partially downregulated in *Six1*$^{-/-}$ embryos (Fig. 6K). To quantify these changes, we performed qRT-PCR using dorsal mandibular arch RNA from control and *Six1*$^{-/-}$ embryos. Supporting the ISH results, expression of *Prrx1* and *Prrx2* in *Six1*$^{-/-}$ embryos was elevated 3-fold, with *Barx1* expression elevated 5-fold (Fig. 6M). *Pou3f3* expression, appearing downregulated in ISH, was 50% lower in qRT-PCR (Fig. 6M). Taken together, these results show that loss of *Six1* causes changes in the patterning of NCCs in the hinge/dorsal mandibular arch domain that are similar to, but less severe than, changes observed in *CBA-Edn1;Wnt1-Cre* animals.

As mentioned above, Prrx1a/b and Barx1 in zebrafish work in parallel with Jagged-Notch and Ednra signaling to establish the timing of chondrogenesis in the first and second arches, thus establishing the hinge region (Barske et al., 2016). Because expression of both *Prrx1* and *Prrx2* expands into the dorsal domain in the absence of SIX1, we examined whether this expansion correlated with precocious ossification in this domain. In E12.5 control embryos, *Osterix* (*Osx*), a transcription factor associated with early osteogenesis (Baek et al., 2013; Nakashima et al., 2002), was weakly expressed in the posterior maxillary region (Fig. 7A). By contrast, loss of SIX1 resulted in an apparent expansion of *Osx* expression in this region (Fig. 7B). Since this domain is likely to give rise to the novel maxillary bone, these findings are consistent with an association between the expansion of these genes and precocious ossification.

DISCUSSION

We have shown here that SIX1 normally represses *Edn1* expression in the endoderm lining of both mandibular arch 1 and the first pharyngeal pouch, thus preventing EDNRA signaling in the adjacent NCC-derived mesenchyme of the dorsal mandibular arch, a region referred to as the hinge in the 'hinge and caps' model of pharyngeal arch development (Depew and Simpson, 2006; Depew et al., 2005; Tavares et al., 2012). At the same time, SIX1 induces Jagged-Notch signaling in the dorsal arch mesenchyme. This places SIX1 temporally upstream of both EDN1 and Jagged-Notch and explains why dorsal ventral patterning is maintained in arch 1 in the absence of Jagged-Notch signaling. Based on the *Six1*$^{-/-}$ phenotype, SIX1 action is essential to limit bone formation in the posterior maxilla during jaw morphogenesis.

Loss of *Six1* causes a partial homeotic transformation of the maxilla

Aberrant EDNRA signaling throughout the first arch following misexpression of *Edn1* in cranial NCCs results in homeotic transformation of the maxilla into a mandible-like structure (Sato et al., 2008a; Tavares and Clouthier, 2015). Although a complete homeotic transformation is not observed in *Six1*$^{-/-}$ embryos, early upregulation of some EDNRA signaling mediators in the dorsal mandibular arch is accompanied by later aberrant expansion of the maxilla posteriorly as a large rod-shaped bone, with its posterior end covered in cartilage. Such a structure is suggestive of a duplication of the proximal portion of the mandible, a hypothesis strengthened by the finding that removing one allele of *Ednra* in a *Six1*$^{-/-}$

Development (2017) 144, 2021-2031 doi:10.1242/dev.145144

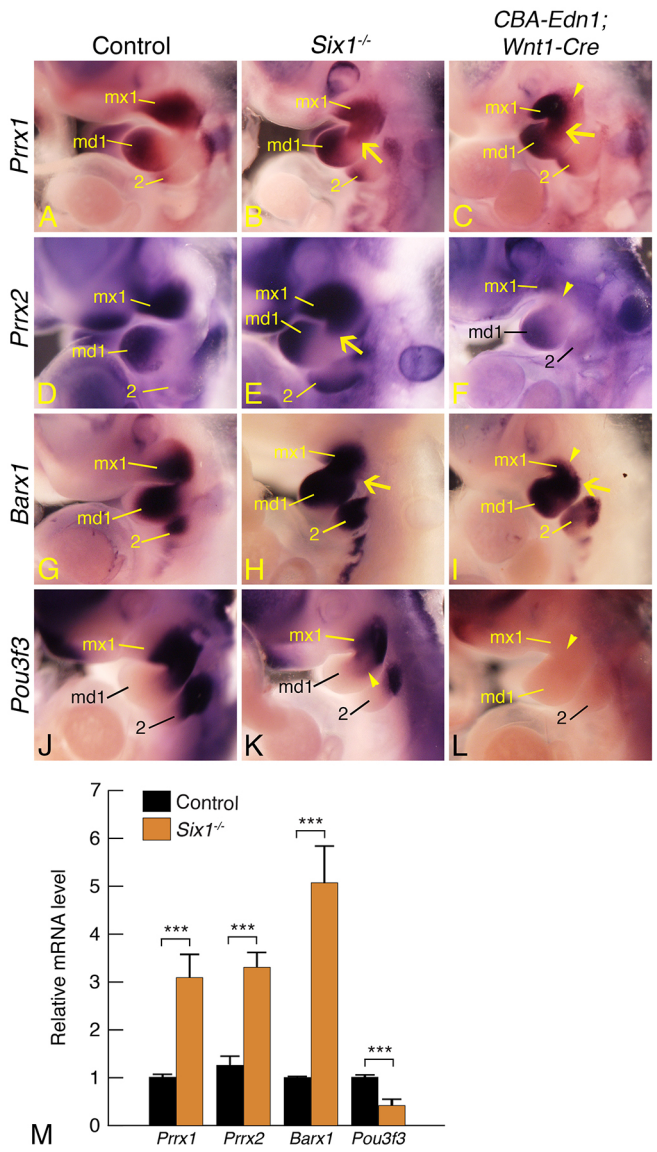

Fig. 6. Expression of early pharyngeal arch patterning genes. (A-L) Whole-mount ISH analysis of *Prrx1*, *Prrx2*, *Barx1* and *Pou3f3* in E10.5 control (A,D,G,J), *Six1*$^{-/-}$ (B,E,H,K) and *CBA-Edn1;Wnt1-Cre* (C,F,I,L) embryos. Arrows denote regions of expanded gene expression; arrowheads denote regions of reduced gene expression. (M) Quantification of *Prrx1*, *Prrx2*, *Barx1* and *Pou3f3* expression in the dorsal mandibular arch of E10.5 control and *Six1*$^{-/-}$ embryos. *n*=3; error bars represent s.e.m.; two-tailed *t*-test, ***P<0.001. md1, mandibular portion of arch 1; mx1, maxillary prominence of arch 1; 2, second pharyngeal arch.

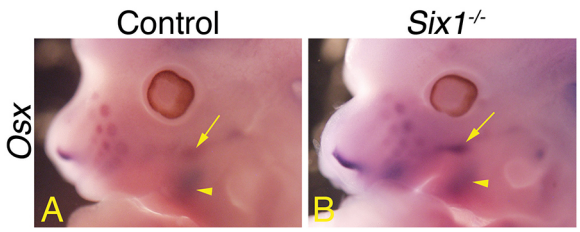

Fig. 7. Upregulation of *Osterix* expression in *Six1*$^{-/-}$ embryos. Whole-mount ISH analysis of *Osterix* (*Osx*) expression in E12.5 control (A) and *Six1*$^{-/-}$ (B) embryos. *Osx* expression is more pronounced in the maxilla of *Six1*$^{-/-}$ embryos (B) than in control embryos (A) (arrows), whereas expression in the mandible appears similar between the two genotypes (arrowheads). The images shown are representative of three embryos of each genotype.

background rescues the craniofacial phenotype in *Six1*$^{-/-}$ embryos. The absence of a complete duplication could be due to the fact that the *Hand2* upregulation observed by qRT-PCR in these embryos is weak compared with that observed in *CBA-Edn1;Wnt1-Cre* embryos. Overexpression of *Hand2* in NCCs, either through expression of *Hand2* from the *Ednra* locus (*Ednra*^{Hand2}) (Sato et al., 2008b) or by overexpressing *Hand2* in NCCs (*Hand2*^{NC}) (Funato et al., 2016), produces a mandible duplication phenotype very similar to that observed following *Edn1* expression in cranial NCCs (Sato et al., 2008a; Tavares and Clouthier, 2015). These findings indicate that ectopic expression of *Hand2* in the maxillary prominence is required and sufficient for complete transformation of the maxilla into a mandible. A similar situation is observed in *jag1b* mutant zebrafish, in which loss of Jagged-Notch signaling does not result in expanded *hand2* expression in the first arch, and dorsal-to-ventral transformation of cartilage elements is not observed (Zuniga et al., 2010). Further studies to understand the mechanism behind repression of *Hand2* in the dorsal arch are required to clarify this point.

SIX1 regulates *Edn1* expression in the dorsal mandibular arch

Jagged-Notch signaling during zebrafish embryogenesis is believed to establish a dorsal arch domain in at least the first and second pharyngeal arches, in part through restricting Ednra signaling to the intermediate domain through mechanisms that function downstream of actual receptor signaling (Alexander et al., 2011; Barske et al., 2016; Zuniga et al., 2011, 2010). However, as discussed above, dorsal-to-ventral transformation of dorsal first arch cartilage derivatives are not observed in *jag1b* mutants, which has led to the hypothesis that Jagged-Notch signaling has a more extensive role in establishing the identity of second arch NCCs (Barske et al., 2016; Zuniga et al., 2010). Defects in arch 1 structures are also not widely observed in mouse embryos in which Jagged-Notch signaling is disrupted. Although conditional loss of *Jag1* in mouse NCCs (*Jag1*$^{fl/fl}$*;Wnt1-Cre* embryos) resulted in shortening of the maxilla, a new posterior extension suggestive of a transformation was not observed (Humphreys et al., 2012). Similarly, the maxilla in embryos with an NCC-specific deletion of *Rbpj* (a molecule responsible for activation of the canonical Notch pathway) appears normal (Mead and Yutzey, 2012). In addition, no gross facial abnormalities were reported in mice containing a neural crest-specific deletion of *Pofut1*, the gene encoding protein *O*-fucosyltransferase 1 (POFUT1), whose modification of Notch is required for Notch signaling (Okamura and Saga, 2008), although detailed skeletal analysis was not presented.

Our current results provide an explanation for these findings: in Jagged-Notch pathway mutants, *Six1* expression in the pharyngeal pouch endoderm is unaffected. Therefore, dorsal *Edn1* expression is repressed, preventing both EDNRA signaling in the dorsal arch and subsequent arch repatterning (Fig. 8). Negative regulation of *Edn1* expression by SIX1 is crucial to maintain dorsal NCC identity; although EDNRA is found in all cranial NCCs (Clouthier et al., 1998), EDN1 is normally derived from the intermediate and ventral ectoderm of the mandibular arch (Clouthier et al., 1998; Yanagisawa et al., 1998; Miller et al., 2000) and has a short half-life and limited diffusion potential (Yanagisawa, 1994). This means that any change in EDNRA signaling in the dorsal mandibular arch would likely require an EDN1 source very close to the dorsal domain. In addition, our *in vitro* data show that EDNRA signaling can block SIX1-induced *Jag1* expression. Thus, these results indicate that while SIX1

Development (2017) 144, 2021-2031 doi:10.1242/dev.145144

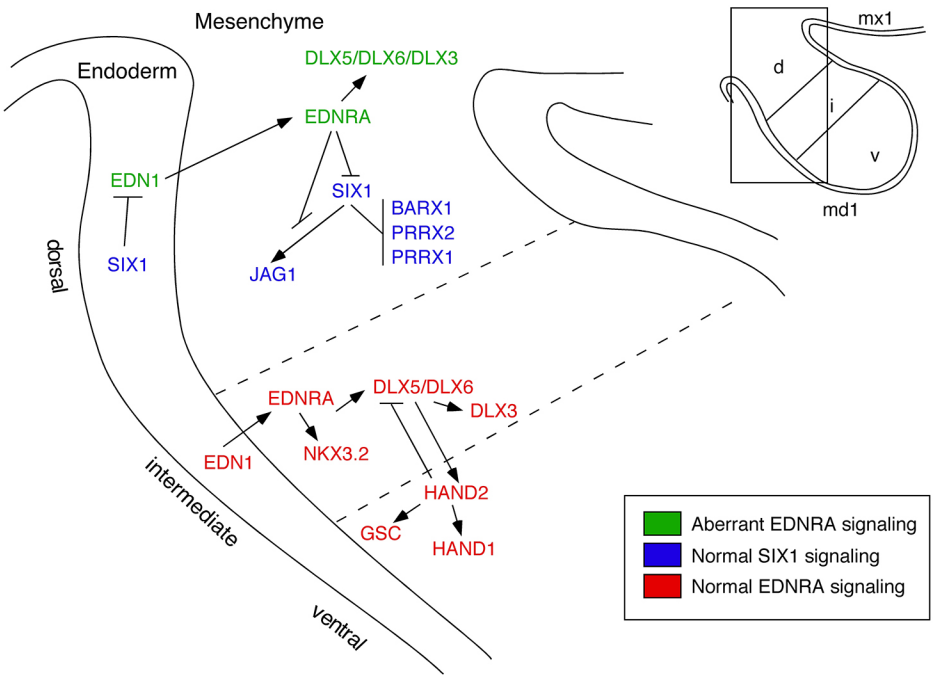

Fig. 8. Model of dorsal (hinge) domain patterning by SIX1. Normal dorsal arch gene expression (represented by *Jag1*) is shown in blue; normal ventral gene expression induced by EDNRA signaling is shown in red. Loss of SIX1 leads to upregulation of EDN1 in the pharyngeal endoderm, which induces EDNRA signaling in the hinge region (shown in green). Subsequent repression of *Jag1* expression by EDNRA signaling compounds loss of SIX1-induced *Jag1* expression. Loss of *Jag1* expression also leads to aberrant expression of genes involved in osteogenesis. While normal EDNRA signaling in the ventral arch and aberrant dorsal arch EDNRA signaling induce similar genes, the source of EDN1 is different for each region.

signaling is crucial for NCC identity in the dorsal mandibular arch, Jagged-Notch signaling by itself is not, at least in mouse. Rather, SIX1-Jagged-Notch signaling ensures that the dorsal mandibular arch domain develops in an EDNRA-independent manner, thus demarcating the mammalian hinge region. This is clearly not the only function of Jagged-Notch signaling, as recent findings illustrate that Jagged-Notch signaling in zebrafish is crucial for later establishment of the sites and timing of arch chondrogenesis (Barske et al., 2016). The role of SIX1 in repressing *Edn1* expression also explains why inactivating one copy of *Ednra* in $Six1^{-/-}$ embryos rescued the phenotype in almost 50% of $Six1^{-/-}$; $Ednra^{+/-}$ embryos. Allelic reduction of *Edn1* gene dosage ($Edn1^{+/-}$) results in a 40% decrease in the expression of both *Dlx5* and *Dlx6* (Vieux-Rochas et al., 2010), indicating that the expression of these two genes is exquisitely sensitive to the level of EDNRA signaling and that decreasing *Ednra* dosage in $Six1^{-/-}$;$Ednra^{+/-}$ embryos is likely to be sufficient to reduce their aberrant expression in the dorsal domain and thus reestablish normal developmental control in this region.

Potential functions of the SIX1-Jagged-Notch signaling axis in the hinge region

The 'hinge and caps' model has been proposed to explain how signals from the ventral arches influence development of more dorsal regions (Britanova et al., 2006; Depew and Compagnucci, 2008; Depew and Simpson, 2006; Depew et al., 2005; Tavares et al., 2012). In mammals, the caps of the first arch encompass the ventral aspects of the mandibular arch and the region surrounding the lambdoidal junction in the maxillary prominence, while the hinge region includes the dorsal portions of both arches and some of the intermediate domain of the mandibular arch (Depew et al., 2005). It is from this region that the TMJ arises (Kontges and Lumsden, 1996). Here we have shown that while the condylar process of the mandible and the mandibular fossa are normal in $Six1^{-/-}$ embryos, the new elongated maxillary bone extends into the mandibular fossa, with the articular disk bifurcating to encompass both the condylar process and the proximal end of the elongated bone. Although bifid mandibular condyle in humans has been reported (Khojastepour et al., 2015; Cho and Jung, 2013) and is observed in $Foxc1^{-/-}$ mouse embryos (Inman et al., 2013), to our knowledge this is the first example of a maxillary bone inserting into the TMJ and associating with the articular disk.

In our current model, SIX1 establishes a dorsal mandibular arch domain by inhibiting endodermal *Edn1* expression, which prevents expansion of Dlx gene expression (Fig. 8). Jagged-Notch signaling induced by SIX1 contributes to this domain by repressing the expression of genes associated with ossification. Such a temporal buffer would thus allow controlled ossification in the maxilla without intrusion into the forming TMJ. This function of Jagged-Notch signaling appears to be conserved in the zebrafish arch, as dorsal expression of *prrx1a/b* and *barx1* is repressed by Jagged-Notch signaling (Barske et al., 2016). However, there are also differences between species, as *Prrx1* and *Barx1* have overlapping expression domains in the mouse mandibular arch, whereas zebrafish *barx1* expression is repressed by *prrx1a/b* (Barske et al., 2016). These differences might relate to different temporal functions, as many of the effects examined in our study occur during early NCC patterning, whereas the studies in zebrafish embryogenesis focused on later chondrogenesis (Barske et al., 2016). However, in mouse models lacking *Prrx1* or both *Prrx1* and *Prrx2*, intramembranous elements of the maxilla and TMJ do not form (Lu et al., 1999; ten Berge et al., 1998), suggesting that PRRX1/2 have roles in pattering the mammalian jaw apparatus.

While we have focused on SIX1 regulation of EDN1 and Jagged-Notch signaling during normal patterning of the dorsal mandibular arch, other molecules function in this region during facial morphogenesis, including FGFs, SHH, TBXs, TGFs and BMPs (reviewed by Chai and Maxson, 2006; Gou et al., 2015; Medeiros and Crump, 2012), with at least some interacting with SIX1 in this process. One example is FGF8, the expression of which in the dorsal mandibular arch is regulated by SIX1/EYA1 action (Guo et al., 2011), while SIX1 and EYA1 regulate GLI activators during development (Eisner et al., 2015). As Wnt signaling acting through R-spondin 2 (RSPO2) has been reported to work in an FGF8/EDN1 pathway during ventral mandibular arch patterning (Jin et al., 2011), it will be interesting to see how these pathways relate to the

Development (2017) 144, 2021-2031 doi:10.1242/dev.145144

establishment or maintenance of the dorsal domain and/or TMJ development.

MATERIALS AND METHODS

Mice

Generation and genotyping of *Wnt1-Cre* (Danielian et al., 1998), *Six1*$^{+/-}$ (Ozaki et al., 2004), *CBA-Edn1* (Tavares and Clouthier, 2015), *Jag1*^{flox} (Brooker et al., 2006) and *Ednra*$^{+/-}$ (Clouthier et al., 1998) mice have been previously described. The *Six1*$^{+/-}$ strain has been backcrossed onto the 129S6 background five generations. The *Ednra*$^{+/-}$ strain has been backcrossed onto the 129S6 background >12 generations. Briefly, *CBA-Edn1* animals carry an *Edn1* expression cassette that is separated from the *CBA* promoter by a strong stop cassette flanked by loxP sites. Breeding these mice with the *Wnt1-Cre* strain results in the removal of the stop cassette and thus expression of *Edn1* in NCCs (Tavares and Clouthier, 2015). The sex of embryos was not determined. All experiments using mice were approved by the Institutional Animal Care and Use Committee (IACUC) at the University of Colorado Anschutz Medical Campus. Care of these mice followed local and national animal welfare law and guidelines. The University of Colorado Anschutz Medical Campus is certified by the Association for Assessment and Accreditation of Laboratory Animal Care.

Skeletal staining

Skeletal staining, analysis and photography of E18.5 embryos with Alizarin Red (bone) and Alcian Blue (cartilage) was performed as previously described (Ruest et al., 2004; Tavares et al., 2012). Four embryos of each genotype were examined for phenotype, with no variation observed between embryos of the same genotype.

Micro-CT and image processing

Embryos were imaged at the Small Animal Tomographic Analysis Facility at Seattle Children's Research Institute using a Skyscan model 1076 micro-computed tomograph (Bruker). Scans were collected at an isotropic resolution of 35.26 µm using the following parameters: no filter, 45 kV, 180 µA, 100 ms exposure, three frame averaging, 0.6° rotation step. All raw data were reconstructed using Nrecon V1.6.9.4 (Bruker) with consistent grayscale thresholding and the smoothing parameters set to 1. Reconstructed data were then rendered and assessed in 3D using Drishti V2.6 Volume Exploration software (Ajay Limaye, 2006; http://sf.anu.edu.au/Vizlab/drishti), again using consistent transfer function parameters to allow for comparison between specimens.

Whole-mount and section ISH

Whole-mount ISH analysis was performed as previously described (Clouthier et al., 1998). To detect bound probe, embryos were incubated in 4-nitro blue tetrazolium chloride (NBT) and 5-bromo-4-chloro-3-indolyl-phosphate (BCIP) (Roche) except when detecting *Six1* and *Osx* expression, where embryos were incubated with BM-Purple (Roche) (Tavares and Clouthier, 2015). Section ISH was performed as previously described (Vincentz et al., 2016). All ISH experiments were performed on a minimum of three mutant embryos. Three to four embryos of each genotype were examined for expression of each marker.

Quantification of the *Hey1* expression domain

Determination of the *Hey1* expression domain in control and *Six1*$^{-/-}$ embryos was performed in a randomized manner. E10.5 embryos were collected, with genotyping performed by a second individual. Four control and four *Six1*$^{-/-}$ embryos were provided for *Hey1* ISH. Following completion of ISH, the area of *Hey1* expression in the dorsal domain of the mandibular arch of all eight embryos was measured using ImageJ (NIH). Genotypes were then revealed and data compiled. Statistical analysis was conducted using Excel (Microsoft), with significance calculated using an unpaired two-tailed *t*-test.

Histology

The collection, staining and analysis of E18.5 embryos were performed as previously described (Barron et al., 2011). Four embryos of each genotype were examined for phenotype, with no variation observed between embryos of the same genotype.

Cell culture

O9-1 cells (Ishii et al., 2012) (EMD Millipore) were cultured on dishes coated with Matrigel in Complete ES Cell Medium (EMD Millipore) supplemented with 25 ng/ml FGF2 (EMD Millipore) at 37°C and 5% CO_2. Cells were only used between passages 2 and 8. Antibiotics and antifungal agents were not used during culture and no signs of contamination were observed.

Six1 overexpression and *in vitro* EDN1 treatment

The *Six1* overexpression plasmid *pfSix1* has been previously described (Ford et al., 1998). An empty pFLAG-CMV-2 vector was used as a control for transfection experiments. O9-1 cells were seeded into 12-well plates and transfected 24 h later. Then, 0.8 µg of either control plasmid or *pfSix1* were transfected into O9-1 cells using X-tremeGENE 9 DNA Transfection Reagent (Sigma-Aldrich). Transfection complexes were made according to the manufacturer's recommendations, added to culture media and incubated for 48 h. In some experiments, EDN1 (Sigma-Aldrich) was added to a final concentration of 10 nM in the culture medium with the transfection complexes. Experiments were performed in duplicate (technical replicate), with each transfection experiment performed three to four times (biological replicate).

RNA collection and qRT-PCR

RNA collection from dissected E9.5 and E10.5 mouse dorsal mandibular arches and from O9-1 cells was performed as previously described (Barron et al., 2011). qRT-PCR was performed using 5 ng cDNA with the Quantitect SYBR Green PCR Kit (Qiagen) and Quantitect assay primers (Qiagen). qRT-PCR of each biological replicate was performed in triplicate. PCR and data analysis were performed using a CFX Connect thermocycler (Bio-Rad). Statistical analysis was conducted using Excel, with significance calculated using an unpaired two-tailed *t*-test.

Acknowledgements

We thank Holly Buttermore and Camilla Teng for technical assistance and Peter Dempsey and the Clouthier/Ford labs for helpful discussions.

Competing interests

The authors declare no competing or financial interests.

Author contributions

Conceptualization: A.L.P.T., D.E.C.; Methodology: A.L.P.T., D.E.C.; Software: T.C.C.; Validation: R.M.M.; Investigation: A.L.P.T.; Resources: T.C.C., R.M.M., H.L.F.; Data curation: A.L.P.T., T.C.C., R.M.M., D.E.C.; Writing - original draft: A.L.P.T., H.L.F., D.E.C.; Writing - review & editing: A.L.P.T., H.L.F., D.E.C.; Visualization: T.C.C., D.E.C.; Supervision: D.E.C.; Project administration: D.E.C.; Funding acquisition: D.E.C.

Funding

This work was supported by the National Institutes of Health (DE018899 and DE023050 to D.E.C. and CA095277 to H.L.F.) and by an endowment for Pediatric Craniofacial Research from the Laurel Foundation (T.C.C.). Deposited in PMC for release after 12 months.

References

Alexander, C., Zuniga, E., Blitz, I. L., Wada, N., Le Pabic, P., Javidan, Y., Zhang, T., Cho, K. W., Crump, J. G. and Schilling, T. F. (2011). Combinatorial roles for Bmps and Endothelin 1 in patterning the dorsal-ventral axis of the craniofacial skeleton. *Development* **138**, 5135-5146.

Baek, W.-Y., Kim, Y.-J., de Crombrugghe, B. and Kim, J.-E. (2013). Osterix is required for cranial neural crest-derived craniofacial bone formation. *Biochem. Biophys. Res. Commun.* **432**, 188-192.

Barron, F., Woods, C., Kuhn, K., Bishop, J., Howard, M. J. and Clouthier, D. E. (2011). Downregulation of *Dlx5* and *Dlx6* expression by Hand2 is essential for initiation of tongue morphogenesis. *Development* **138**, 2249-2259.

Barske, L., Askary, A., Zuniga, E., Balczerski, B., Bump, P., Nichols, J. T. and Crump, J. G. (2016). Competition between Jagged-Notch and Endothelin1 signaling selectively restricts cartilage formation in the zebrafish upper face. *PLoS Genet.* **12**, e1005967.

Development (2017) 144, 2021-2031 doi:10.1242/dev.145144

Bosman, E. A., Quint, E., Fuchs, H., Hrabé de Angelis, M. and Steel, K. P. (2009). Catweasel mice: a novel role for Six1 in sensory patch development and a model for branchio-oto-renal syndrome. *Dev. Biol.* **328**, 285-296.

Britanova, O., Depew, M. J., Schwark, M., Thomas, B. L., Miletich, I., Sharpe, P. T. and Tarabykin, V. (2006). *Satb2* haploinsufficiency phenocopies 2q32-q33 deletions, whereas loss suggests a fundamental role in the coordination of jaw development. *Am. J. Hum. Genet.* **79**, 668-678.

Brooker, R., Hozumi, K. and Lewis, J. (2006). Notch ligands with contrasting functions: Jagged1 and Delta1 in the mouse inner ear. *Development* **133**, 1277-1286.

Chai, Y. and Maxson, R. E., Jr. (2006). Recent advances in craniofacial morphogenesis. *Dev. Dyn.* **235**, 2353-2375.

Cho, B.-H. and Jung, Y.-H. (2013). Nontraumatic bifid mandibular condyles in asymptomatic and symptomatic temporomandibular joint subjects. *Imaging Sci. Dent.* **43**, 25-30.

Clouthier, D. E. and Schilling, T. F. (2004). Understanding endothelin-1 function during craniofacial development in the mouse and zebrafish. *Birth Defects Res. C* **72**, 190-199.

Clouthier, D. E., Hosoda, K., Richardson, J. A., Williams, S. C., Yanagisawa, H., Kuwaki, T., Kumada, M., Hammer, R. E. and Yanagisawa, M. (1998). Cranial and cardiac neural crest defects in endothelin-A receptor-deficient mice. *Development* **125**, 813-824.

Clouthier, D. E., Williams, S. C., Yanagisawa, H., Wieduwilt, M., Richardson, J. A. and Yanagisawa, M. (2000). Signaling pathways crucial for craniofacial development revealed by endothelin-A receptor-deficient mice. *Dev. Biol.* **217**, 10-24.

Clouthier, D. E., Garcia, E. and Schilling, T. F. (2010). Regulation of facial morphogenesis by endothelin signaling: insights from mice and fish. *Am. J. Med. Genet. A* **152A**, 2962-2973.

Clouthier, D. E., Passos-Bueno, M. R., Tavares, A. L. P., Lyonnet, S., Amiel, J. and Gordon, C. T. (2013). Understanding the basis of Auriculocondylar syndrome: Insights from human, mouse and zebrafish genetic studies. *Am. J. Med. Genet C* **163**, 306-317.

Danielian, P. S., Muccino, D., Rowitch, D. H., Michael, S. K. and McMahon, A. P. (1998). Modification of gene activity in mouse embryos in utero by a tamoxifen-inducible form of Cre recombinase. *Curr. Biol.* **8**, 1323-1326.

Depew, M. J. and Compagnucci, C. (2008). Tweaking the hinge and caps: testing a model of the organization of jaws. *J. Exp. Zool.* **310B**, 315-335.

Depew, M. J. and Simpson, C. A. (2006). 21st century neonatology and the comparative development of the vertebrate skull. *Dev. Dyn.* **235**, 1256-1291.

Depew, M. J., Simpson, C. A., Morasso, M. and Rubenstein, J. L. R. (2005). Reassessing the *Dlx* code: the genetic regulation of branchial arch skeletal pattern and development. *J. Anat.* **207**, 501-561.

Eisner, A., Pazyra-Murphy, M. F., Durresi, E., Zhou, P., Zhao, X., Chadwick, E. C., Xu, P.-X., Hillman, R. T., Scott, M. P., Greenberg, M. E. et al. (2015). The Eya1 phosphatase promotes Shh signaling during hindbrain development and oncogenesis. *Dev. Cell* **33**, 22-35.

Ford, H. L., Kabingu, E. N., Bump, E. A., Mutter, G. L. and Pardee, A. B. (1998). Abrogation of the G2 cell cycle checkpoint associated with overexpression of HSIX1: a possible mechanism of breast carcinogenesis. *Proc. Natl. Acad. Sci. USA* **95**, 12608-12613.

Funato, N., Kokubo, H., Nakamura, M., Yanagisawa, H. and Saga, Y. (2016). Specification of jaw identity by the Hand2 transcription factor. *Sci. Rep.* **6**, 28405.

Gou, Y., Zhang, T. and Xu, J. (2015). Transcription factors in craniofacial development: from receptor signaling to transcriptional and epigenetic regulation. *Curr. Top. Dev. Biol.* **115**, 377-410.

Guo, C., Sun, Y., Zhou, B., Adam, R. M., Li, X. K., Pu, W. T., Morrow, B. E., Moon, A. and Li, X. (2011). A *Tbx1-Six1/Eya1-Fgf8* genetic pathway controls mammalian cardiovascular and craniofacial morphogenesis. *J. Clin. Invest.* **121**, 1585-1595.

Hanken, J. and Hall, B. K. (ed.) (1993). *The Skull*. Chicago: University of Chicago Press.

Humphreys, R., Zheng, W., Prince, L. S., Qu, X., Brown, C., Loomes, K., Huppert, S. S., Baldwin, S. and Goudy, S. (2012). Cranial neural crest ablation of *Jagged1* recapitulates the craniofacial phenotype of Alagille syndrome patients. *Hum. Mol. Genet.* **21**, 1374-1383.

Ikeda, K., Kageyama, R., Suzuki, Y. and Kawakami, K. (2010). Six1 is indispensable for production of functional progenitor cells during olfactory epithelial development. *Int. J. Dev. Biol.* **54**, 1453-1464.

Inman, K. E., Purcell, P., Kume, T. and Trainor, P. A. (2013). Interaction between Foxc1 and Fgf8 during mammalian jaw patterning and in the pathogenesis of syngnathia. *PLoS Genet.* **9**, e1003949.

Ishii, M., Arias, A. C., Liu, L., Chen, Y.-B., Bronner, M. E. and Maxson, R. E. (2012). A stable cranial neural crest cell line from mouse. *Stem Cells Dev.* **21**, 3069-3080.

Jin, Y.-R., Turcotte, T. J., Crocker, A. L., Han, X. H. and Yoon, J. K. (2011). The canonical Wnt signaling activator, R-spondin2, regulates craniofacial patterning and morphogenesis within the branchial arch through ectodermal-mesenchymal interaction. *Dev. Biol.* **352**, 1-13.

Kawakami, K., Sato, S., Ozaki, H. and Ikeda, K. (2000). *Six* family genes–structure and function as transcription factors and their roles in development. *BioEssays* **22**, 616-626.

Khojastepour, L., Kolahi, S., Panahi, N. and Haghnegahdar, A. (2015). Cone beam computed tomographic assessment of bifid mandibular condyle. *J. Dent. (Tehran)* **12**, 868-873.

Kimmel, C. B., Ullmann, B., Walker, M., Miller, C. T. and Crump, J. G. (2003). Endothelin 1-mediated regulation of pharyngeal bone development in zebrafish. *Development* **130**, 1339-1351.

Kontges, G. and Lumsden, A. (1996). Rhombencephalic neural crest segmentation is preserved throughout craniofacial ontogeny. *Development* **122**, 3229-3242.

Kumar, J. P. (2009). The sine oculis homeobox (SIX) family of transcription factors as regulators of development and disease. *Cell Mol. Life Sci.* **66**, 565-583.

Laclef, C., Souil, E., Demignon, J. and Maire, P. (2003). Thymus, kidney and craniofacial abnormalities in *Six1* deficient mice. *Mech. Dev.* **120**, 669-679.

Le Douarin, N. M. (1982). *The Neural Crest*. New York: Cambridge University Press.

Lee, K. Y., Kim, S. H., Kim, U. K., Ki, C.-S. and Lee, S. H. (2007). Novel EYA1 mutation in a Korean branchio-oto-renal syndrome family. *Int. J. Pediatr. Otorhinolaryngol.* **71**, 169-174.

Lu, M. F., Cheng, H. T., Kern, M. J., Potter, S. S., Tran, B., Diekwisch, T. G. and Martin, J. F. (1999). *prx-1* functions cooperatively with another *paired*-related homeobox gene, *prx-2*, to maintain cell fates within the craniofacial mesenchyme. *Development* **126**, 495-504.

Mead, T. J. and Yutzey, K. E. (2012). Notch pathway regulation of neural crest cell development in vivo. *Dev. Dyn.* **241**, 376-389.

Medeiros, D. M. and Crump, J. G. (2012). New perspectives on pharyngeal dorsoventral patterning in development and evolution of the vertebrate jaw. *Dev. Biol.* **371**, 121-135.

Miller, C. T., Schilling, T. F., Lee, K.-H., Parker, J. and Kimmel, C. B. (2000). *sucker* encodes a zebrafish Endothelin-1 required for ventral pharyngeal arch development. *Development* **127**, 3815-3838.

Miller, C. T., Yelon, D., Stainier, D. Y. and Kimmel, C. B. (2003). Two *endothelin 1* effectors, *hand2* and *bapx1*, pattern ventral pharyngeal cartilage and the jaw joint. *Development* **130**, 1353-1365.

Nair, S., Li, W., Cornell, R. and Schilling, T. F. (2007). Requirements for endothelin type-A receptors and endothelin-1 signaling in the facial ectoderm for the patterning of skeletogenic neural crest cells in zebrafish. *Development* **134**, 335-345.

Nakashima, K., Zhou, X., Kunkel, G., Zhang, Z., Deng, J. M., Behringer, R. R. and de Crombrugghe, B. (2002). The novel zinc finger-containing transcription factor osterix is required for osteoblast differentiation and bone formation. *Cell* **108**, 17-29.

Nichols, J. T., Pan, L., Moens, C. B. and Kimmel, C. B. (2013). *barx1* represses joints and promotes cartilage in the craniofacial skeleton. *Development* **140**, 2765-2775.

Noden, D. M. (1983). The role of the neural crest in patterning of avian cranial skeletal, connective, and muscle tissues. *Dev. Biol.* **96**, 144-165.

Okamura, Y. and Saga, Y. (2008). Notch signaling is required for the maintenance of enteric neural crest progenitors. *Development* **135**, 3555-3565.

Orten, D. J., Fischer, S. M., Sorensen, J. L., Radhakrishna, U., Cremers, C. W. R. J., Marres, H. A. M., Van Camp, G., Welch, K. O., Smith, R. J. H. and Kimberling, W. J. (2008). Branchio-oto-renal syndrome (BOR): novel mutations in the *EYA1* gene, and a review of the mutational genetics of BOR. *Hum. Mutat.* **29**, 537-544.

Ozaki, H., Nakamura, K., Funahashi, J.-I., Ikeda, K., Yamada, G., Tokano, H., Okamura, H.-O., Kitamura, K., Muto, S., Kotaki, H. et al. (2004). Six1 controls patterning of the mouse otic vesicle. *Development* **131**, 551-562.

Ozeki, H., Kurihara, Y., Tonami, K., Watatani, S. and Kurihara, H. (2004). Endothelin-1 regulates the dorsoventral branchial arch patterning in mice. *Mech. Dev.* **121**, 387-395.

Ruest, L.-B., Xiang, X., Lim, K. C., Levi, G. and Clouthier, D. E. (2004). Endothelin-A receptor-dependent and -independent signaling pathways in establishing mandibular identity. *Development* **131**, 4413-4423.

Ruf, R. G., Berkman, J., Wolf, M. T., Nurnberg, P., Gattas, M., Ruf, E. M., Hyland, V., Kromberg, J., Glass, I., Macmillan, J. et al. (2003). A gene locus for branchio-otic syndrome maps to chromosome 14q21.3-q24.3. *J. Med. Genet.* **40**, 515-519.

Ruf, R. G., Xu, P.-X., Silvius, D., Otto, E. A., Beekmann, F., Muerb, U. T., Kumar, S., Neuhaus, T. J., Kemper, M. J., Raymond, R. M., Jr. et al. (2004). SIX1 mutations cause branchio-oto-renal syndrome by disruption of EYA1-SIX1-DNA complexes. *Proc. Natl. Acad. Sci. USA* **101**, 8090-8095.

Sato, T., Kawamura, Y., Asai, R., Amano, T., Uchijima, Y., Dettlaff-Swiercz, D. A., Offermanns, S., Kurihara, Y. and Kurihara, H. (2008a). Recombinase-mediated cassette exchange reveals the selective use of Gq/G11-dependent and -independent endothelin 1/endothelin type A receptor signaling in pharyngeal arch development. *Development* **135**, 755-765.

Sato, T., Kurihara, Y., Asai, R., Kawamura, Y., Tonami, K., Uchijima, Y., Heude, E., Ekker, M., Levi, G. and Kurihara, H. (2008b). An endothelin-1 switch

specifies maxillomandibular identity. *Proc. Natl. Acad. Sci. USA* **105**, 18806-18811.

Smith, A. L., Iwanaga, R., Drasin, D. J., Micalizzi, D. S., Vartuli, R. L., Tan, A.-C. and Ford, H. L. (2012). The miR-106b-25 cluster targets Smad7, activates TGF-beta signaling, and induces EMT and tumor initiating cell characteristics downstream of Six1 in human breast cancer. *Oncogene* **31**, 5162-5171.

Talbot, J. C., Johnson, S. L. and Kimmel, C. B. (2010). *hand2* and Dlx genes specify dorsal, intermediate and ventral domains within zebrafish pharyngeal arches. *Development* **137**, 2507-2517.

Tavares, A. L. P. and Clouthier, D. E. (2015). Cre recombinase-regulated Endothelin1 transgenic mouse lines: novel tools for analysis of embryonic and adult disorders. *Dev. Biol.* **400**, 191-201.

Tavares, A. L. P., Garcia, E. L., Kuhn, K., Woods, C. M., Williams, T. and Clouthier, D. E. (2012). Ectodermal-derived Endothelin1 is required for patterning the distal and intermediate domains of the mouse mandibular arch. *Dev. Biol.* **371**, 47-56.

ten Berge, D., Brouwer, A., Korving, J., Martin, J. F. and Meijlink, F. (1998). *Prx1* and *Prx2* in skeletogenesis: roles in the craniofacial region, inner ear and limbs. *Development* **125**, 3831-3842.

Vieux-Rochas, M., Mantero, S., Heude, E., Barbieri, O., Astigiano, S., Couly, G., Kurihara, H., Levi, G. and Merlo, G. R. (2010). Spatio-temporal dynamics of gene expression of the Edn1-Dlx5/6 pathway during development of the lower jaw. *Genesis* **48**, 262-373.

Vincentz, J. W., Casasnovas, J. J., Barnes, R. M., Que, J., Clouthier, D. E., Wang, J. and Firulli, A. B. (2016). Exclusion of *Dlx5*/*6* expression from the distal-most mandibular arches enables BMP-mediated specification of the distal cap. *Proc. Natl. Acad. Sci. USA* **113**, 7563-7568.

Walker, M. B., Miller, C. T., Talbot, J. C., Stock, D. W. and Kimmel, C. B. (2006). Zebrafish *furin* mutants reveal intricacies in regulating Endothelin1 signaling in craniofacial patterning. *Dev. Biol.* **295**, 194-205.

Xu, P.-X., Zheng, W., Huang, L., Maire, P., Laclef, C. and Silvius, D. (2003). Six1 is required for the early organogenesis of mammalian kidney. *Development* **130**, 3085-3094.

Yanagisawa, M. (1994). The endothelin system: a new target for therapeutic intervention. *Circulation* **89**, 1320-1322.

Yanagisawa, H., Hammer, R. E., Richardson, J. A., Williams, S. C., Clouthier, D. E. and Yanagisawa, M. (1998). Role of Endothelin-1/Endothelin-A receptor-mediated signaling pathway in the aortic arch patterning in mice. *J. Clin. Invest.* **102**, 22-33.

Zou, D., Silvius, D., Fritzsch, B. and Xu, P. X. (2004). Eya1 and Six1 are essential for early steps of sensory neurogenesis in mammalian cranial placodes. *Development* **131**, 5561-5572.

Zou, D., Silvius, D., Davenport, J., Grifone, R., Maire, P. and Xu, P.-X. (2006). Patterning of the third pharyngeal pouch into thymus/parathyroid by Six and Eya1. *Dev. Biol.* **293**, 499-512.

Zuniga, E., Stellabotte, F. and Crump, J. G. (2010). Jagged-Notch signaling ensures dorsal skeletal identity in the vertebrate face. *Development* **137**, 1843-1852.

Zuniga, E., Rippen, M., Alexander, C., Schilling, T. F. and Crump, J. G. (2011). Gremlin 2 regulates distinct roles of Bmp and Endothelin 1 signaling in dorsoventral patterning of the facial skeleton. *Development* **138**, 5147-5156.